Pramana – J. Phys. (2019) 93:28
https://doi.org/10.1007/s12043-019-1773-8

Numerical simulation of space-fractional Helmholtz equation arising in seismic wave propagation, imaging and inversion

AMIT PRAKASH[1,*], MANISH GOYAL[2] and SHIVANGI GUPTA[2]

[1]Department of Mathematics, National Institute of Technology, Kurukshetra 136 119, India
[2]Department of Mathematics, Institute of Applied Sciences and Humanities, GLA University, Mathura 281 406, India
[*]Corresponding author. E-mail: amitmath@nitkkr.ac.in, amitmath0185@gmail.com

MS received 3 July 2018; revised 18 December 2018; accepted 4 January 2019; published online 23 May 2019

Abstract. In this paper, a reliable numerical scheme, the q-fractional homotopy analysis transform method (q-FHATM), is proposed to examine the Helmholtz equation of fractional order arising in seismic wave propagation, imaging and inversion. Sufficient conditions for its convergence and error estimates are established. The q-FHATM provides a solution in a rapidly convergent series. Results for different fractional values of space derivatives are compared with the existing methods and discussed with the help of figures. A proper selection of parameters yields approximations identical to the exact solution. Parameter $\hbar$ offers an expedient way of controlling the region of convergence of the solution. Test examples are provided to illustrate the accuracy and competency of the proposed scheme. The outcomes divulge that our scheme is attractive, user-friendly, reliable and highly effective.

Keywords. Fractional Helmholtz equation; q-fractional homotopy analysis transform method; fractional variation iteration method; Caputo fractional derivative.

PACS Nos 02.60.−Cb; 05.45.−a

1. Introduction

In the past few decades, fractional-order calculus has emerged as a potential tool in various domains of science and engineering such as fluid dynamic traffic, neurophysiology [1], potential theory, control theory, viscoelasticity, electromagnetic theory, bioengineering, electric technology, plasma physics and mathematical economy. Real-world processes, which we deal with, are normally of fractional order. Heat diffusion into a semi-infinite solid where heat flow equals the half-derivative of the temperature is an example of a fractional-order system.

Mass–energy equation of Einstein is obtained with the conjecture of absolute smooth space–time but space–time is congenitally discontinuous if it tends to a quantum scale. A Hilbert cube can model actual fractal space–time. The discontinuity of space–time may be shown if we reckon a TV image smooth at all noticeable scales. But, if the scale inclines to a very small one, the image becomes unsmooth and involves many arrayed pixels. So, time becomes discontinuous when it is tremendously small. A film provides 24 slips/s. It gives a continuous movement but for 10 slips/s, movement converts to a discontinuous one. Then for discontinuous space–time, the fractal theory is embraced to define numerous phenomena [2]. Molecular diffusion in water is similar to stochastic Brownian motion considering continuum mechanics but the diffusion follows fractal Fick laws if motion is noticed on a molecular scale. Water flow gets discontinuous and fractal calculus is needed to define molecular motion that gets entirely unpredictable in the continuum mechanics frame. The heat-proof property of a cocoon cannot be divulged by advanced calculus. If the wall of the cocoon is thought of as a continuous medium, it is hard to explain why the temperature changes in its inner surface, very slowly, irrespective of the environmental temperature [3]. Time turns discontinuous in microphysics and so fractal kinetics takes place on a very small time scale. In a smooth nanofibre membrane, if we study the effects of diameter of the nanofibres on air permeability, we use a nanoscale as the nanofibre membrane turns discontinuous and fractal calculus is effectively used [4].

Differential equations which govern systems with memory are fractional differential equations (FDEs).

Arbitrariness in their order introduces more degrees of freedom in design and analysis, resulting in more accurate modelling, better robustness in control and greater flexibility in signal processing. Electrochemical phenomena such as double-layer charge distribution or the diffusion process can be better explained with a fractional-order system. As a result, the modelling of lithium in batteries, fuel cells and supercapacitors are carried out with FDEs. The characterisation of ceramic bodies, fractal structures, viscoelastic materials, decay rate of fruits and meat and the study of corrosion in metal surfaces are also promising areas of their applications. Fractional-order system is also a popular choice to study real-time events such as earthquake propagation, volcanic phenomenon, design of thermokinetics, modelling of human lungs and skin. Even characteristics of economic market fluctuation adopt fractional calculus-based system modelling. So, fractional-order analysis is changed from an inert physical network to a living network of biology, ecology, physiology and sociology, reminding us Leibnitz's prediction in his letter to L'Hopital in 1695 that the fractional differential operator is 'an apparent paradox from which one day useful consequences will be drawn'.

In the frequency domain, the Helmholtz equation is a version of an acoustic wave equation. It is used in imaging and seismic wave propagation. Its numerical solution is significant for forward modelling in geophysical frequency domain inversion [5]. Its two-dimensional form appears in water wave propagation, acoustic radiation, heat conduction, steady-state-related problems, biology and governing equation in waveguide problems. It has a vital role in the pattern formation of animal coating, prediction of acoustic propagation in shallow water at low frequencies, estimation of geodesic sea floor properties [6], etc.

The Helmholtz equation is derived from wave equation and its nature is elliptic. In a two-dimensional non-homogeneous isotropic medium with speed c, wave solution is $u(x, y)$ corresponding to a harmonic source $\psi(x, y)$ which vibrates at a fixed frequency $\omega > 0$ and satisfies the Helmholtz equation in the region R. Integer-order Helmholtz equation is

$$D_x^2 u(x, y) + D_y^2 u(x, y) + \varepsilon u(x, y) = -\psi(x, y). \tag{1}$$

Here, u is a sufficiently differentiable function on the boundary of R, ψ is a given function, $\varepsilon > 0$ is constant while $\sqrt{\varepsilon} = (\omega/c)$ is the wave number with wavelength $2\pi/\sqrt{\varepsilon}$. $\psi = 0$ makes eq. (1) homogeneous. If eq. (1) is written as

$$D_x^2 u(x, y) + D_y^2 u(x, y) - \varepsilon u(x, y) = -\psi(x, y), \tag{2}$$

then it describes mass transfer processes with volume chemical reactions of first order. Equation (1) is studied using finite element method [7], decomposition method [8], Trefftz method [9], differential transform method [10], spectral collocation method [11], etc.

The biggest advantage of using fractional models of differential equations in physical models is their non-local property. Fractional-order derivative is non-local while integer-order derivative is local in nature. It shows that the upcoming state of the physical system is also dependent on all its historical states in addition to its present state. Hence, the fractional models are more realistic. In FDEs, response expression has a parameter which describes the variable order of the fractional derivative that may be varied to achieve several responses.

Standard Helmholtz equations can be generalised to Helmholtz equation of fractional order by the extension of the integer-order space derivative to the Caputo fractional space derivative. Space fractional Helmholtz equation is

$$D_x^\alpha u(x, y) + D_y^2 u(x, y) + \varepsilon u(x, y) = -\psi(x, y) \tag{3}$$

with $u(0, y) = \xi(y)$ as the initial condition. Gupta *et al* [12] used homotopy perturbation method to solve multidimensional fractional Helmholtz equation while Abuasad *et al* [13] recently applied reduced differential transform method to solve a fractional model of Helmholtz equation. This model has not yet been studied by q-fractional homotopy analysis transform method (q-FHATM) and fractional variation iteration method (FVIM).

Space fractional derivatives arise for heavy tailed variations. They describe the motion of a particle that accounts for the flow field variation over the whole system. Fractional equations describe motion of particle with memory in time. Fraction in derivative suggests the modulation of system memory. It is apparent that seismic wave propagation is influenced by variations in flow field. This fact marks fractional modelling suitable for such phenomenon. Hence the study of space-fractional Helmholtz equations is very important.

From the physical perspective, it is sensible to have a fractional derivative of a constant equal to zero. For the Riemann–Liouville fractional operator, $D_t^\alpha c = (c/\Gamma(1-\alpha))t^{-\alpha} \neq 0, c =$ constant while for the Caputo fractional operator, ${}_a^C D_t^\alpha c = 0, c =$ constant. A great advantages of the Caputo fractional derivatives is that it allows traditional initial and boundary conditions to be included in the formulation of the problem. Now, consider the following initial value problem (IVP):

$$D^\alpha y(t) - \lambda\, y(t) = 0, \quad t > 0, \quad n-1 < \alpha < n;$$
$$y^k(0) = b_k, \quad k = 0, \ldots, n-1.$$

In this problem, where the Caputo fractional operator is applicable, standard initial conditions in terms of derivatives of integer order are involved. These initial conditions have obvious physical interpretations as an initial position $y(a)$ at point a, initial velocity $y'(a)$ initial acceleration $y''(a)$ and so on. To compute the fractional derivative of a function in Caputo sense, it requires the existence of the nth derivative of a function. Luckily, most functions that appear in applications fulfil this prerequisite. Caputo fractional derivative is defined only for differentiable functions and we have considered u as a sufficiently differentiable function in this paper.

Most nonlinear FDEs do not possess the exact solutions, and so some numerical techniques are required for their approximate numerical solution. Reliability of solution schemes is also a very important aspect compared to modelling dimensions of equations [14,15]. FVIM [16] directly attacks the nonlinear FDEs without the need to find certain polynomials for nonlinear terms and gives results in an infinite series that rapidly converges to analytical solution. This method does not require linearisation, discretisation, little perturbations or any restrictive assumptions. It lessens mathematical computations significantly. FVIM has a thoroughness in the mathematical derivation of the Lagrangian multiplier by variational theory for fractional calculus. It leads to a solution converging to the exact one. Recently, fractional complex transform [17] was developed to build a simpler variational iteration algorithm for fractional calculus. Baleanu *et al* [18] applied local fractional variational iteration transform method on nonlinear gas dynamics and coupled KdV equations having a local fractional operator to obtain a non-differentiable solution. A complete review on applications of FVIM is available in [19].

The usual analytical methods need more memory in the computer as well as time for computation. So, to overcome these limitations, the analytical methods are to be amalgamated with transform operators to work on nonlinear equations [2,20–22]. The q-FHATM [23] is an elegant union of q-homotopy analysis method (q-HAM) and transform of Laplace. Liao [24] presented HAM in which an incessant mapping is formed from initial speculation to exact solution after selecting auxiliary linear operator. Solution convergence is confirmed by the auxiliary parameter. The q-HAM is actually an improvement of parameter $q \in [0, 1]$ in HAM to $q \in [0, (1/n)], n \geq 1$. The superiority of q-FHATM is its potential of adjusting two strong computational methodologies for probing FDEs.

The aim of this paper is to obtain a numerical solution of a space-fractional model of Helmholtz equation by q-FHATM and compare our results with existing techniques. This paper is structured in the following manner. Section 1 is introduction. In §2, we give a brief review of the preliminary description of Caputo fractional derivative, Mittag–Leffler function and some other results, helpful for investigating FDEs. In §3, the basic plan of the proposed numerical method q-FHATM is shown by taking the problem under consideration. In §4, the basic plan of FVIM is provided. Convergence of q-FHATM and FVIM are discussed along with its implementation on the given model and numerical test examples. Section 5 deals with the discussion of the obtained numerical results and their significance. In §6, we recapitulate our outcomes and draw inferences.

2. Preliminaries

DEFINITION 1

Consider a real function $h(\chi)$, $\chi > 0$. It is called in space

a. $C_\zeta, \zeta \in R$ if $\exists$ a real number $b\,(>\zeta)$, s.t. $h(\chi) = \chi^b h_1(\chi)$, $h_1 \in C[0, \infty)$. Clearly $C_\zeta \subset C_\gamma$ if $\gamma \leq \zeta$.
b. $C_\zeta^m, m \in \mathbb{N} \cup \{0\}$ if $h^{(m)} \in C_\zeta$.

DEFINITION 2 [24]

The Caputo fractional derivative of h, $h \in C_{-1}^m, m \in \mathbb{N} \cup \{0\}$ is

$$D_t^\beta h(t) = \begin{cases} I^{m-\beta} h^{(m)}(t), & m-1 < \beta < m, \quad m \in \mathbb{N}, \\ \frac{\mathrm{d}^m}{\mathrm{d}t^m} h(t), & \beta = m, \end{cases}$$

a. $I_t^\zeta h(x,t) = \dfrac{1}{\Gamma\zeta} \displaystyle\int_0^t (t-s)^{\zeta-1} h(x,s)\mathrm{d}s, \quad \zeta, t > 0,$

b. $D_\tau^\nu V(x,\tau) = I_\tau^{m-\nu} \dfrac{\partial^m V(x,\tau)}{\partial t^m}, \quad m-1 < \nu \leq m,$

c. $D_t^\zeta I_t^\zeta h(t) = h(t), \quad m-1 < \zeta \leq m, \quad m \in \mathbb{N},$

d. $I_t^\zeta D_t^\zeta h(t) = h(t) - \displaystyle\sum_{k=1}^{m-1} h^k(0^+) \frac{t^k}{k!},$

$$m-1 < \zeta \leq m, \quad m \in \mathbb{N}.$$

e. $I^v t^\zeta = \dfrac{\Gamma(\zeta+1)}{\Gamma(v+\zeta+1)} t^{v+\zeta}.$

DEFINITION 3 [24]

Laplace transform of the Caputo fractional derivative is

$$L[D^\alpha g(t)] = p^\alpha L[g(t)] - \sum_{k=0}^{n-1} p^{\alpha-k-1} g^{(k)}(0^+),$$

$$n-1 < \alpha \leq n.$$

DEFINITION 4 [24]

Mittag–Leffler function is demarcated by the given series representation valid in the entire complex plane:

$$E_\zeta(z) = \sum_{m=0}^{\infty} (z^m / \Gamma(1 + \zeta m)), \quad \zeta > 0, \quad z \in C.$$

3. Proposed q-FHATM for space-fractional Helmholtz equation

Let us ponder over a space-fractional nonlinear non-homogeneous PDE

$$\begin{aligned} &D_x^\alpha u(x, y) + Ru(x, y) + Nu(x, y) = g(x, y), \\ &n - 1 < \alpha \leq n, \end{aligned} \tag{4}$$

where R and N are linear and nonlinear operators, respectively, and $g(x, y)$ is the source term.

Taking the transform of Laplace on each side of eq. (4) and then simplifying, we obtain

$$\begin{aligned} L[u(x, y)] &- \frac{1}{p^\alpha} \sum_{k=0}^{n-1} p^{\alpha-k-1} u^k(0, y) \\ &+ \frac{1}{p^\alpha}[L\{Ru(x, y) + Nu(x, y) - g(x, y)\}] = 0. \end{aligned} \tag{5}$$

The nonlinear operator is formulated as

$$\begin{aligned} N[\phi(x, y; q)] &= L[\phi(x, y; q)] \\ &- \frac{1}{p^\alpha} \sum_{k=0}^{n-1} p^{\alpha-k-1} \phi^k(x, y; q)(0^+) \\ &+ \frac{1}{p^\alpha}\{L[R\phi(x, y; q) + N\phi(x, y; q)]\} \\ &- \frac{1}{p^\alpha}\{L[g(x, y)]\}. \end{aligned} \tag{6}$$

$q \in [0, \frac{1}{n}]$ is the embedding parameter and $\phi(x, y; q)$ is a real-valued function.

We build homotopy [25,26] as

$$\begin{aligned} &(1 - nq)L[\phi(x, y; q) - u_0(x, y)] \\ &= \hbar q H(x, y) N[\phi(x, y; q)], \quad n \geq 1 \end{aligned} \tag{7}$$

where $H \neq 0$ is an auxiliary function, $\hbar \neq 0$ is an auxiliary parameter, u_0 is the initial value and ϕ is an unknown function.

For $q = 0$ and $\frac{1}{n}$, the ensuing results hold:

$$\phi(x, y; 0) = u_0(x, y), \quad \phi\left(x, y; \frac{1}{n}\right) = u(x, y). \tag{8}$$

Consequently, as q increases from 0 to $1/n, n \geq 1$, $\phi(x, y; q)$ changes from u_0 to solution $u(x, y)$. Applying Taylor's theorem on ϕ to expand it about q, we get

$$\phi(x, y; q) = u_0(x, y) + \sum_{m=1}^{\infty} u_m(x, y) q^m, \tag{9}$$

where

$$u_m(x, y) = \frac{1}{m!} \frac{\partial^m \phi(x, y; q)}{\partial q^m}\bigg|_{q=0}. \tag{10}$$

For suitable choice of auxiliary operators, u_0, $n, \hbar$ and H, series (9) converges at $q = 1/n$, and we obtain

$$u(x, y) = u_0(x, y) + \sum_{m=1}^{\infty} u_m(x, y) \left(\frac{1}{n}\right)^m. \tag{11}$$

Express the vectors as

$$\vec{u}_m = \{u_0(x, y), u_1(x, y), \ldots, u_m(x, y)\}. \tag{12}$$

Differentiate deformation eq. (7) of the zeroth order m times and divide by $m!$. Finally taking $q = 0$, deformation equation of order m is obtained as

$$L[u_m(x, y) - k_m u_{m-1}(x, y)] = \hbar H(x, y) æ_m(\vec{u}_{m-1}). \tag{13}$$

Taking the inverse transform, we get

$$\begin{aligned} u_m(x, y) &= k_m u_{m-1}(x, y) \\ &+ \hbar L^{-1}[H(x, y) æ_m(\vec{u}_{m-1})]. \end{aligned} \tag{14}$$

In eq. (14), we express $æ_m(\vec{u}_{m-1})$ in a new manner as

$$\begin{aligned} æ_m(\vec{u}_{m-1}) &= Lu_{m-1}(x, y) - \left(1 - \frac{k_m}{n}\right) \\ &\times \left[\frac{1}{p^\alpha} \sum_{k=0}^{n-1} p^{\alpha-k-1} u^k(0, y) + \frac{1}{p^\alpha} L\{g(x, y)\}\right] \\ &+ \frac{1}{p^\alpha} L\{Ru_{m-1}(x, y) + P_{m-1}\} \end{aligned} \tag{15}$$

and k_m is represented as

$$k_m = \begin{cases} 0, & m \leq 1, \\ n, & m > 1. \end{cases} \tag{16}$$

In eq. (15), P_m is the homotopy polynomial which is expressed as

$$P_m = \frac{1}{m!}\left[\frac{\partial^m \phi(x, y; q)}{\partial q^m}\right]\bigg|_{q=0} \tag{17}$$

and

$$\phi = \phi_0 + q\phi_1 + q^2\phi_2 + \cdots. \tag{18}$$

Using results of eqs (15) into (14), we get

$$u_m(x, y) = (k_m + \hbar)u_{m-1}(x, y) - \hbar\left(1 - \frac{k_m}{n}\right)L^{-1} \times \left[\frac{1}{p^\alpha}\sum_{k=0}^{n-1} p^{\alpha-k-1}\, u^k(0, y) + \frac{1}{p^\alpha}L\{g(x, y)\}\right] + \hbar L^{-1}\left[\frac{1}{p^\alpha}L[Ru_{m-1}(x, y) + P_{m-1}]\right]. \quad (19)$$

The advancement in this recommended procedure is that an innovative correction function (19) is established by applying homotopy polynomials.

Eventually from eq. (19), components $u(x, y)$ for $m \geq 1$ can be computed using Maple package.

Subsequently, the q-FHATM solution is

$$u(x, y) = \sum_{m=1}^{\infty} u_m(x, y)\left(\frac{1}{n}\right)^m. \quad (20)$$

Theorem [24]. *If* $\exists$ *a constant* $0 < \chi < 1$ *s.t.*$\|\zeta_{m+1}(t)\| \leq \chi \|\zeta_m(t)\| \forall m$ *and if truncated series* $\sum_{m=0}^{r} \zeta_m(t)(1/n)^m$ *is used as the approximate solution* $\zeta(t)$, *then maximum absolute truncation error is found as*

$$\left\| \zeta(t) - \sum_{m=0}^{r} \zeta_m(t)(1/n)^m \right\| \leq (\chi^{r+1}/n^r(n - \chi))\, \|\zeta_0(t)\|.$$

3.1 *Implementation of q-FHATM*

Now we show the applicability of q-FHATM via a few test examples.

Example 1. Consider an x-space fractional Helmholtz equation:

$$D_x^\alpha u(x, y) + D_y^2 u(x, y) - u(x, y) = 0, \quad 1 < \alpha \leq 2 \quad (21)$$

with the starting condition

$$u(0, y) = y. \quad (22)$$

Exact solution of eqs (21) and (22) for $\alpha = 2$ is

$$u = y \cosh x. \quad (23)$$

Using the transform of Laplace on each side of eq. (21) and simplifying, we get

$$L[u] - \frac{y}{p} + \frac{1}{p^\alpha} L[u_{yy} - u] = 0. \quad (24)$$

We state the nonlinear operator as

$$N[\phi(x, y; q)] = L[\phi(x, y; q)] - \left(1 - \frac{k_m}{n}\right)\frac{y}{p} + \frac{1}{p^\alpha} L[D_y^2 \phi(x, y; q) - \phi(x, y; q)]. \quad (25)$$

Deformation equation for $H(x, y) = 1$ is written as

$$L[u_m(x, y) - k_m u_{m-1}(x, y)] = \hbar æ_m(\vec{u}_{m-1}). \quad (26)$$

Here

$$æ_m(\vec{u}_{m-1}) = L[u_{m-1}] - \left(1 - \frac{k_m}{n}\right)\frac{y}{p} + \frac{1}{p^\alpha} L[D_y^2 u_{m-1} - u_{m-1}].$$

Taking the inverse transform, we get

$$u_m(x, y) = k_m u_{m-1}(x, y) + \hbar L^{-1}\, æ_m(\vec{u}_{m-1}). \quad (27)$$

Simplification yields the following approximations of the q-FHATM solution:

$$u_0 = y,$$
$$u_1 = \frac{-\hbar y x^\alpha}{\Gamma(1 + \alpha)},$$
$$u_2 = \frac{-(\hbar + n)\hbar y x^\alpha}{\Gamma(1 + \alpha)} + \frac{\hbar^2 y x^{2\alpha}}{\Gamma(1 + 2\alpha)},$$
$$u_3 = \frac{-(\hbar + n)^2 \hbar y x^\alpha}{\Gamma(1 + \alpha)} + \frac{2(\hbar + n)\hbar^2 y x^{2\alpha}}{\Gamma(1 + 2\alpha)} - \frac{\hbar^3 y x^{3\alpha}}{\Gamma(1 + 3\alpha)} + \cdots,$$

and so on.

Persisting in this way, next iterations $u_m(x, y)$, $m \geq 4$ can be achieved using Maple package.

Then, the solution is expressed as

$$u(x, y) = u_0 + \sum_{m=1}^{\infty} u_m(x, y)\left(\frac{1}{n}\right)^m. \quad (28)$$

It is observed that if $\alpha = 2, \hbar = -1,\ n = 1$, the series solution $\sum_{m=0}^{N} u_m(x, y)(1/n)^m$ converges to the exact solution (23) as $N \to \infty$,

$$u(x, y) = y\left[1 + \frac{x^\alpha}{\Gamma(1 + \alpha)} + \frac{x^{2\alpha}}{\Gamma(1 + 2\alpha)} + \frac{x^{3\alpha}}{\Gamma(1 + 3\alpha)} + \frac{x^{4\alpha}}{\Gamma(1 + 4\alpha)} + \cdots\right] = y\sum_{k=0}^{\infty} \frac{x^{k\alpha}}{\Gamma(1 + k\alpha)} = y E_\alpha(x^\alpha),$$

where $E_\alpha(z)$ is the Mittag–Leffler function.

Example 2. Consider another x-space fractional homogeneous Helmholtz equation with $\varepsilon = 5$:

$$D_x^{\alpha} u(x,\ y) + D_y^2 u(x,\ y) + 5u(x,\ y) = 0,\quad 1 < \alpha \leq 2, \tag{29}$$

with

$$u(0,\ y) = y \tag{30}$$

as the initial condition. The exact solution of eqs (29) and (30) for $\alpha = 2$ is

$$u = y \cos \sqrt{5}x. \tag{31}$$

Using the transform of Laplace on each side of eq. (29) and using (30), we get

$$L[u] - \frac{y}{p} + \frac{1}{p^{\alpha}} L[u_{yy} + 5u] = 0. \tag{32}$$

We state the nonlinear operator as

$$\begin{aligned} &N[\phi(x,\ y;\ q)] \\ &\quad = L[\phi(x,\ y;\ q)] - \left(1 - \frac{k_m}{n}\right)\frac{y}{p} \\ &\qquad + \frac{1}{p^{\alpha}} L[D_y^2 \phi(x,\ y;\ q) + 5\,\phi(x,\ y;\ q)]. \end{aligned} \tag{33}$$

Deformation equation for $H(x,\ y) = 1$ is

$$L[u_m(x,\ y) - k_m u_{m-1}(x,\ y)] = \hbar æ_m(\vec{u}_{m-1}), \tag{34}$$

where

$$\begin{aligned} æ_m(\vec{u}_{m-1}) &= L[u_{m-1}] - \left(1 - \left(\frac{k_m}{n}\right)\right)\left(\frac{y}{p}\right) \\ &\quad + \left(\frac{1}{p^{\alpha}}\right) L[D_y^2\, u_{m-1} + 5u_{m-1}]. \end{aligned}$$

Taking the inverse transform, we get

$$u_m = k_m u_{m-1} + \hbar L^{-1}\, æ_m(\vec{u}_{m-1}). \tag{35}$$

Simplification yields the following approximations of the q-FHATM solution:

$$\begin{aligned} u_0 &= y, \\ u_1 &= \frac{5\hbar y x^{\alpha}}{\Gamma(1+\alpha)}, \\ u_2 &= \frac{5(\hbar+n)\hbar y x^{\alpha}}{\Gamma(1+\alpha)} + \frac{25\hbar^2 y x^{2\alpha}}{\Gamma(1+2\alpha)}, \\ u_3 &= \frac{5(\hbar+n)^2\hbar y x^{\alpha}}{\Gamma(1+\alpha)} + \frac{50(\hbar+n)\hbar^2 y x^{2\alpha}}{\Gamma(1+2\alpha)} \\ &\quad + \frac{125\,\hbar^3 y x^{3\alpha}}{\Gamma(1+3\alpha)} + \cdots, \end{aligned}$$

and so on.

Persisting in this way, next iterations $u_m(x,\ y)$, $m \geq 4$ can be achieved using Maple package.

Then, the solution is expressed as

$$u(x,\ y) = u_0 + \sum_{m=1}^{\infty} u_m(x,\ y)\left(\frac{1}{n}\right)^m. \tag{36}$$

If $\alpha = 2, \hbar = -1, n = 1$, series solution $\sum_{m=0}^{N} u_m \left(\frac{1}{n}\right)^m$ converges to solution (31) as $N \to \infty$,

$$\begin{aligned} u(x,\ y) &= y\Bigg[1 - \frac{5x^{\alpha}}{\Gamma(1+\alpha)} + \frac{25x^{2\alpha}}{\Gamma(1+2\alpha)} \\ &\qquad - \frac{125x^{3\alpha}}{\Gamma(1+3\alpha)} + \frac{625x^{4\alpha}}{\Gamma(1+4\alpha)} + \cdots\Bigg] \\ &= y E_{\alpha}(-5\,x^{\alpha}). \end{aligned}$$

Example 3. Consider an inhomogeneous two-dimensional fractional Helmholtz equation with $\varepsilon = -2$:

$$\begin{aligned} &D_x^{\alpha} u(x,\ y) + D_y^2 u(x,\ y) - 2u(x,\ y) \\ &\quad = (12x^2 - 3x^4)\sin y, \\ &\qquad 1 < \alpha \leq 2,\ 0 < x \leq 1,\ 0 < y \leq 2\pi \end{aligned} \tag{37}$$

with the starting condition

$$u(0,\ y) = (x^4 - (x^6/10))\sin y. \tag{38}$$

Exact solution of eqs (37) and (38) for $\alpha = 2$ is

$$u = x^4 \sin y. \tag{39}$$

Using the transform of Laplace on each side of eq. (37) and simplifying, we get

$$\begin{aligned} &L[u] - \frac{y}{p} + \frac{1}{p^{\alpha}} L[u_{yy} - 2u - (12x^2 - 3x^4)\sin y] \\ &= 0. \end{aligned} \tag{40}$$

We state the nonlinear operator as

$$\begin{aligned} &N[\phi(x,\ y;\ q)] \\ &\quad = L[\phi(x,\ y;\ q)] - \left(1 - \frac{k_m}{n}\right)\frac{y}{p} \\ &\qquad + \frac{1}{p^{\alpha}} L\Bigg[\frac{\partial^2 \phi(x,\ y;\ q)}{\partial y^2} - 2\,\phi(x,\ y;\ q) \\ &\qquad - (12x^2 - 3x^4)\sin y\Bigg]. \end{aligned} \tag{41}$$

Deformation equation for $H(x,\ y) = 1$ is

$$L[u_m(x,\ y) - k_m u_{m-1}(x,\ y)] = \hbar æ_m(\vec{u}_{m-1}) \tag{42}$$

where

$$\begin{aligned} æ_m(\vec{u}_{m-1}) &= L[u_{m-1}] - (1 - (k_m/n))\frac{y}{p} \\ &\quad + \frac{1}{p^{\alpha}} L[(\partial^2 u_{m-1}/\partial y^2) - 2u_{m-1} \\ &\quad - (12x^2 - 3\,x^4)\sin y]. \end{aligned}$$

Taking the inverse transform, we get

$$u_m = k_m u_{m-1} + \hbar L^{-1} æ_m(\vec{u}_{m-1}). \tag{43}$$

Simplification yields the following approximations of the q-FHATM solution:

$$\begin{aligned}
u_0 &= \left(x^4 - \frac{x^6}{10}\right)\sin y,\\
u_1 &= \frac{-24\hbar \sin y x^{2+\alpha}}{\Gamma(3+\alpha)} + \frac{216\,\hbar \sin y x^{6+\alpha}}{\Gamma(7+\alpha)},\\
u_2 &= -\frac{(1+\hbar+n)24\hbar \sin y x^{2+\alpha}}{\Gamma(3+\alpha)} + \frac{72\,\hbar \sin y x^{4+\alpha}}{\Gamma(5+\alpha)}\\
&\quad + \frac{216(\hbar+n)\hbar \sin y x^{6+\alpha}}{\Gamma(7+\alpha)}\\
&\quad + \frac{72\hbar^2 \sin y x^{2+2\alpha}}{\Gamma(3+2\alpha)} - \frac{648\,\hbar^2 \sin y x^{6+2\alpha}}{\Gamma(7+2\alpha)},\\
u_3 &= -\frac{(1+\hbar+n)24\hbar\, n \sin y x^{2+\alpha}}{\Gamma(3+\alpha)}\\
&\quad + \frac{72\hbar n \sin y x^{4+\alpha}}{\Gamma(5+\alpha)}\\
&\quad + \frac{216\,(\hbar+n)\hbar\, n \sin y x^{6+\alpha}}{\Gamma(7+\alpha)}\\
&\quad + \frac{72\,\hbar^2 n \sin y x^{2+2\,\alpha}}{\Gamma(3+2\alpha)} - \frac{1296\,\hbar^2 n \sin y x^{6+2\alpha}}{\Gamma(7+2\alpha)}\\
&\quad - \frac{(1+\hbar+\hbar^2+\hbar n)24\hbar \sin y x^{2+\alpha}}{\Gamma(3+\alpha)}\\
&\quad + \frac{72(1+\hbar)\,\hbar \sin y x^{4+\alpha}}{\Gamma(5+\alpha)}\\
&\quad + \frac{216(\hbar+n)\hbar^2\, n \sin y x^{6+\alpha}}{\Gamma(7+\alpha)}\\
&\quad + \frac{72(1+2\,\hbar+n)\hbar^2 \sin y x^{2+2\alpha}}{\Gamma(3+2\alpha)}\\
&\quad + \frac{216\,\hbar^2 \sin y x^{4+2\alpha}}{\Gamma(5+2\alpha)} + \frac{1296\hbar^3 \sin y x^{6+2\alpha}}{\Gamma(7+2\alpha)}\\
&\quad - \frac{216\,\hbar^3 \sin y x^{2+3\alpha}}{\Gamma(3+3\alpha)} + \frac{1944\hbar^3 \sin y x^{6+3\alpha}}{\Gamma(7+3\alpha)}\\
&\quad + \cdots.
\end{aligned}$$

Persisting in this way, next iterations $u_m(x, y), m \geq 4$ can be achieved using Maple package.

The solution is expressed as

$$u(x, y) = u_0 + \sum_{m=1}^{\infty} u_m(x, y)\left(\frac{1}{n}\right)^m. \tag{44}$$

4. Proposed FVIM for space-fractional Helmholtz equation

Consider the mathematical model described by eq. (3) as

$$\begin{aligned}
&D_x^\alpha u(x, y) + D_y^2 u(x, y) + \varepsilon\, u(x, y) = -\varphi(x, y);\\
&u(0, y) = y.
\end{aligned}$$

A correction functional is built for eq. (3) as

$$\begin{aligned}
u_{n+1}(x, y) = u_n(x, y) + \int_0^x \lambda(&D_\xi^\alpha u(\xi, y)\\
&+ D_y^2 \tilde{u}_n(\xi, y) + \varepsilon \tilde{u}_n(\xi, y)\\
&+ \varphi(\xi, y))(\mathrm{d}\xi)^\alpha,
\end{aligned} \tag{45}$$

where λ is the Lagrange multiplier. By variational theory, λ must satisfy

$$\left.\frac{\mathrm{d}^\alpha \lambda}{\mathrm{d}\xi^\alpha}\right|_{\xi=x} = 0 \quad \text{and} \quad 1 + \lambda|_{\xi=x} = 0.$$

We quickly get $\lambda = -1$. Then, using it in eq. (3), we get

$$\begin{aligned}
u_{n+1}(x, y) = u_n(x, y) - \int_0^x (&D_\xi^\alpha u_n(\xi, y)\\
&+ D_y^2 u_n(\xi, y) + \varepsilon u_n(\xi, y)\\
&+ \varphi(\xi, y))(\mathrm{d}\xi)^\alpha.
\end{aligned} \tag{46}$$

Consecutive approximations $u_n(x, y), n \geq 0$ can be built henceforth. u_n is a restricted variation, i.e. $\delta\tilde{u}_n = 0$. Finally, we obtain sequences $u_{n+1}(x, y), n \geq 0$ of the solution.

Consequently, the exact solution is obtained as

$$u(x, y) = \lim_{n\to\infty} u_n(x, y). \tag{47}$$

4.1 *Convergence analysis of FVIM*

Now, our emphasis is on the convergence of FVIM applied to eq. (3). Sufficient conditions for the convergence of FVIM and its error estimate are provided.

We define the operator S as

$$\begin{aligned}
S = \int_0^x (-1)(&D_\xi^\alpha u_n(\xi, y) + D_y^2 u_n(\xi, y)\\
&+ \varepsilon u_n(\xi, y) + \varphi(\xi, y))(\mathrm{d}\xi)^\alpha.
\end{aligned} \tag{48}$$

Also, we define the components $v_k, k = 0, 1, 2, \ldots,$ as

$$u(x, y) = \lim_{n\to\infty} u_n(x, y) = \sum_{k=0}^{\infty} v_k. \tag{49}$$

Theorem 1 [27]. *Let S, defined in eq.* (48)*, be an operator from Banach space B to B. Solution as defined in eq.* (49)*, converge if* $0 < q < 1$ *exists such that*

$$\|S[v_0 + v_1 + v_2 + \cdots + v_{k+1}]\| \leq q\|S[v_0 + v_1 + v_2 + \cdots + v_k]\|,$$

(*i.e.* $\|v_{k+1}\| \leq q\|v_k\|$), $\forall\, k \epsilon \mathbb{N} \cup \{0\}$. *It is an exceptional case of Banach fixed point theorem applied in* [28] *as a sufficient condition to discuss FVIM convergence for various equations.*

Theorem 2 [27]. *If the solution defined in eq.* (49) *converges, it is an exact solution of eq.* (3).

Theorem 3 [27]. *Suppose the series solution defined in eq.* (49) *converges to solution* $u(x, y)$ *of problem* (3). *If the truncated series* $\sum_{k=0}^{j} v_k$ *is used as an approximation to* $u(x, y)$ *of eq.* (3)*, then max. error* $E_j(x, y)$ *is assessed as*

$$E_j(x, y) \leq \frac{1}{1-q} q^{j+1} \|v_0\|.$$

If $\forall i \in \mathbb{N} \cup \{0\}$, we state parameters,

$$\chi_i = \begin{cases} \left(\dfrac{\|v_{i+1}\|}{\|v_i\|}\right), & \|v_i\| \neq 0. \\ 0, & \|v_i\| = 0. \end{cases}$$

Then solution $\sum_{k=0}^{\infty} v_k$ of eq. (3) converges to the exact solution $u(x, y)$ when $0 \leq \chi_i < 1, \forall i \in \mathbb{N} \cup \{0\}$.

Also, the maximum absolute truncation error is projected as

$$\left\| u(x, y) - \sum_{k=0}^{\infty} v_k \right\| \leq \frac{1}{1-\chi} \chi^{j+1} \|v_0\|,$$

where $\chi = \max\{\chi_i,\ i = 0,\ 1,\ 2, \ldots, j\}$.

Remark 1 [27]. If first finite χ_i's, $i = 1, 2, \ldots, j$ are not less than 1 and $\chi_i \leq 1, i > j$ then, obviously the series solution $\sum_{k=0}^{\infty} v_k$ of eq. (3) converges to the exact solution. It means that the first finite terms do not affect the convergence of the series solution. FVIM convergence depends on $\chi_i, i > j$.

4.2 *Implementation of FVIM*

Now, we validate the applicability of FVIM through examples.

Example 4. Using condition (22), we initialise with $u_0 = y$ and applying FVIM to eq. (21), we get

$$\begin{aligned} u_1(x, y) &= u_0 - \int_0^x \{D_\xi^\alpha u_0(\xi, y) \\ &\quad + D_y^2 u_0(\xi, y) - u_0(\xi, y)\}(\mathrm{d}\xi)^\alpha \\ &= y + \frac{yx^\alpha}{\Gamma(1+\alpha)}, \\ u_2(x, y) &= y + \frac{yx^\alpha}{\Gamma(1+\alpha)} + \frac{yx^{2\alpha}}{\Gamma(1+2\alpha)}, \\ u_3(x, y) &= y + \frac{yx^\alpha}{\Gamma(1+\alpha)} + \frac{yx^{2\alpha}}{\Gamma(1+2\alpha)} \\ &\quad + \frac{yx^{3\alpha}}{\Gamma(1+3\alpha)} + \cdots. \end{aligned}$$

Proceeding in this way, rest of the components may be obtained using Maple package.

The final solution is

$$u(x, y) = \lim_{n \to \infty} u_n(x, y). \tag{50}$$

In view of eqs (48) and (49), iteration formulae for eq. (3) are

$$\begin{aligned} v_0 &= y, \\ v_1 &= \frac{yx^\alpha}{\Gamma(1+\alpha)}, \\ v_2 &= \frac{yx^{2\alpha}}{\Gamma(1+2\alpha)}, \\ v_3 &= \frac{y\,x^{3\alpha}}{\Gamma(1+3\alpha)}, \\ &\ldots, \\ v_k &= \frac{y\,x^{k\alpha}}{\Gamma(1+k\alpha)}. \end{aligned}$$

Visibly, we conclude that the obtained solution, $\sum_{k=0}^{\infty} v_k$ converges to the exact solution $u = yE_\alpha(x^\alpha)$.

In addition, by computing χ_i's for this problem, we have

$$\chi_i = \frac{\|v_{i+1}\|}{\|v_i\|} = \left\| x^\alpha \frac{\Gamma(1+i\alpha)}{\Gamma(1+(i+1)\alpha)} \right\| < 1$$

when, for example, $i > 1$ and $1 < \alpha \leq 2$. This confirms that the variational approach for problem (3) gives positive and bounded solution that converges to the exact solution.

Remark 2 [27]. The above test problem is taken when $0 < x \leq 1$ to discuss the convergence condition. Still, we may stretch the interval and examine the convergence condition after ignoring the first few terms of the series solution.

For space-fractional Helmholtz equation (3), when $0 < x \leq a$ and $\alpha = 2, a > 0$, then

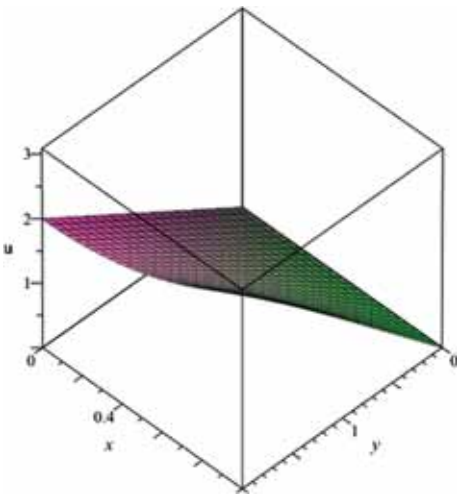

Figure 1. q-FHATM solution (Example 1).

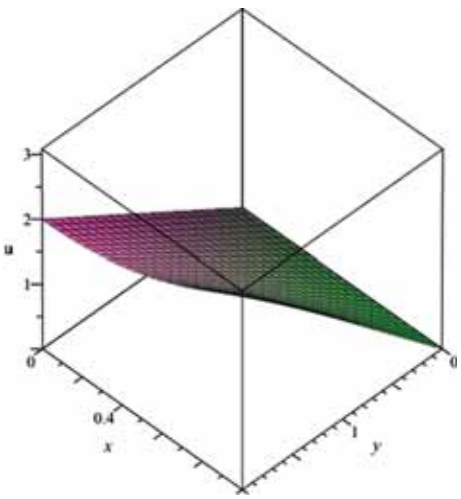

Figure 2. FVIM solution (Example 4).

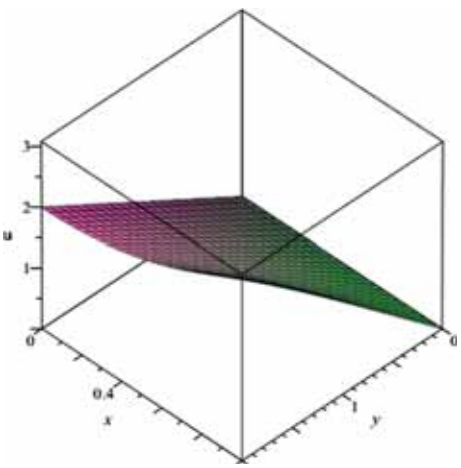

Figure 3. Exact solution (Example 1).

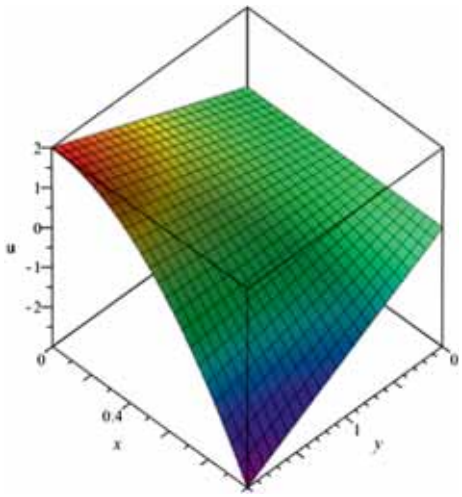

Figure 4. q-FHATM solution (Example 2).

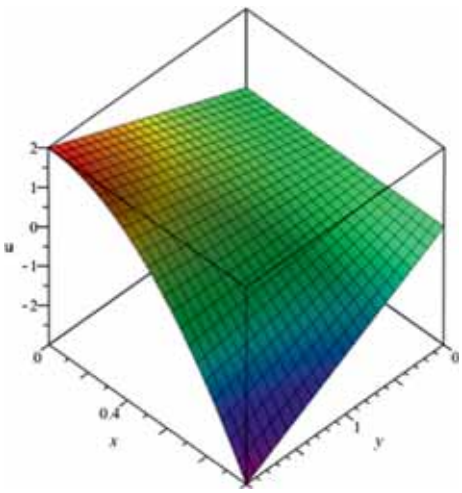

Figure 5. FVIM solution (Example 5).

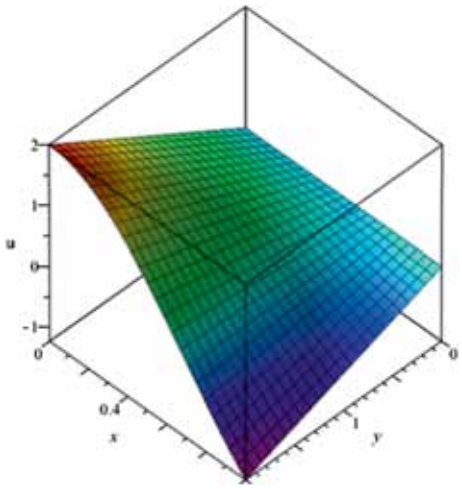

Figure 6. Exact solution (Example 2).

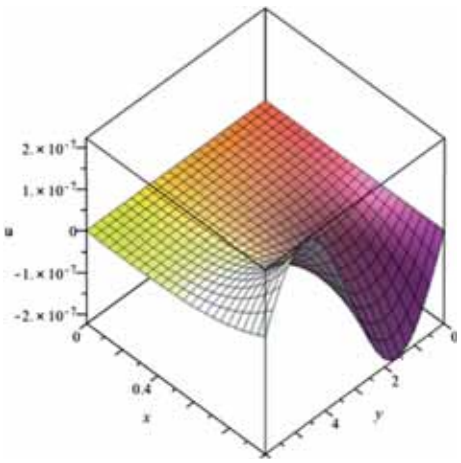

Figure 7. q-FHATM solution (Example 3).

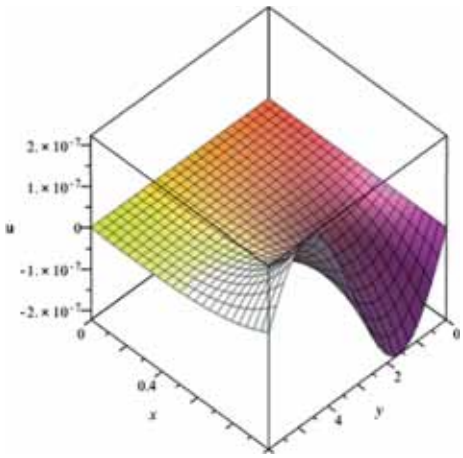

Figure 8. FVIM solution (Example 6).

$$\chi_i = \left\| x^2 \frac{\Gamma(1+2i)}{\Gamma(1+2(i+1))} \right\| \leq \frac{a^2}{(2i+1)(2i+2)} < 1, \quad \text{for } i > a.$$

Example 5. We initialise with $u_0 = y$ and applying FVIM to eq. (29), we get

$$\begin{aligned} u_1(x,y) &= u_0 - \int_0^x \{D_\xi^\alpha u_0(\xi,y) \\ &\quad + D_y^2 u_0(\xi,y) + 5u_0(\xi,y)\}(\mathrm{d}\xi)^\alpha \\ &= y - \frac{5yx^\alpha}{\Gamma(1+\alpha)}, \\ u_2(x,y) &= y - \frac{5yx^\alpha}{\Gamma(1+\alpha)} + \frac{25yx^{2\alpha}}{\Gamma(1+2\alpha)}, \\ u_3(x,y) &= y - \frac{5yx^\alpha}{\Gamma(1+\alpha)} + \frac{25yx^{2\alpha}}{\Gamma(1+2\alpha)} \\ &\quad - \frac{125yx^{3\alpha}}{\Gamma(1+3\alpha)}, \end{aligned}$$

and so on.

Proceeding in the same way, at last, we get the solution

$$u(x,y) = \lim_{n\to\infty} u_n(x,y). \tag{51}$$

Example 6. We initialise with

$$u_0 = (x^4 - (x^6/10))\sin y$$

and apply FVIM to eq. (37), and we get

$$\begin{aligned} u_1(x,y) &= u_0 - \int_0^x \{D_\xi^\alpha u_0(\xi,y) + D_y^2 u_0(\xi,y) \\ &\quad - 2u_0(\xi,y) - (12\xi^2 - 3\xi^4)\sin y\}(\mathrm{d}\xi)^\alpha, \\ &= \left(x^4 - \frac{x^6}{10}\right)\sin y + \frac{24\sin yx^{2+\alpha}}{\Gamma(3+\alpha)} \\ &\quad - \frac{216\sin yx^{6+\alpha}}{\Gamma(7+\alpha)}, \\ u_2(x,y) &= \left(x^4 - \frac{x^6}{10}\right)\sin y + \frac{24\sin yx^{2+\alpha}}{\Gamma(3+\alpha)} \\ &\quad - \frac{216\sin yx^{6+\alpha}}{\Gamma(7+\alpha)} + \frac{72\sin yx^{2+2\alpha}}{\Gamma(3+2\alpha)} \\ &\quad - \frac{648\sin yx^{6+2\alpha}}{\Gamma(7+2\alpha)}, \\ u_3(x,y) &= \left(x^4 - \frac{x^6}{10}\right)\sin y + \frac{24\sin yx^{2+\alpha}}{\Gamma(3+\alpha)} \\ &\quad - \frac{216\sin yx^{6+\alpha}}{\Gamma(7+\alpha)} + \frac{72\sin yx^{2+2\alpha}}{\Gamma(3+2\alpha)} \\ &\quad - \frac{648\sin yx^{6+2\alpha}}{\Gamma(7+2\alpha)} + \frac{216\sin yx^{2+3\alpha}}{\Gamma(3+3\alpha)}, \\ &\quad - \frac{1944\sin yx^{6+3\alpha}}{\Gamma(7+3\alpha)} + \cdots. \end{aligned}$$

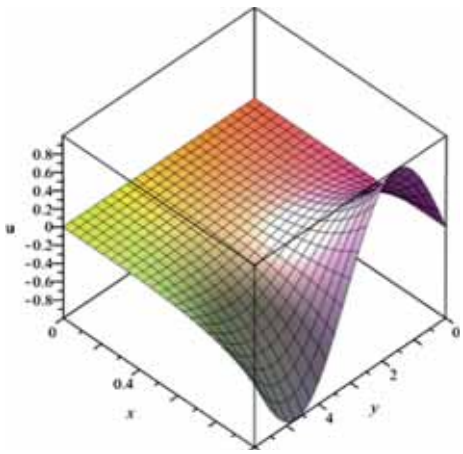

Figure 9. Exact solution (Example 3).

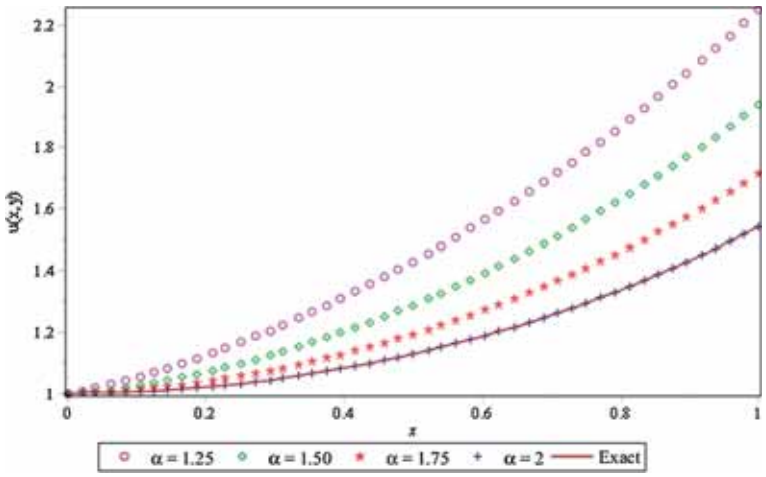

Figure 10. Behaviour of exact and q-FHATM solutions for distinct α when $y = 1 = n, \hbar = -1$ for Example 1.

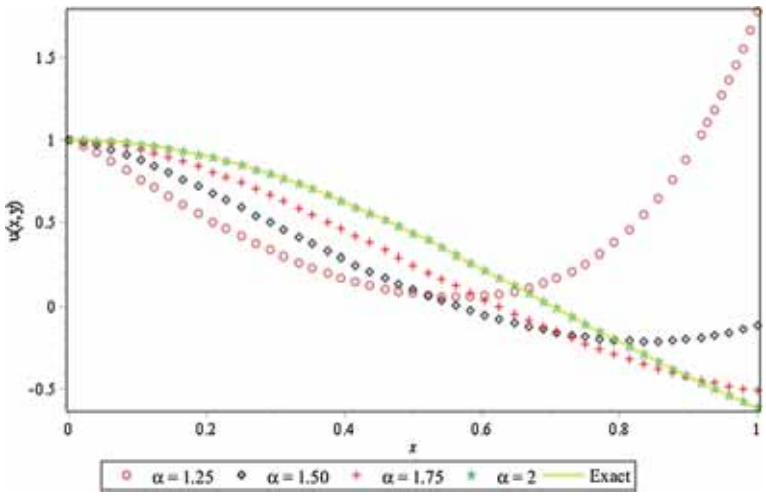

Figure 11. Behaviour of exact and q-FHATM solutions for distinct α when $y = 1 = n, \hbar = -1$ for Example 2.

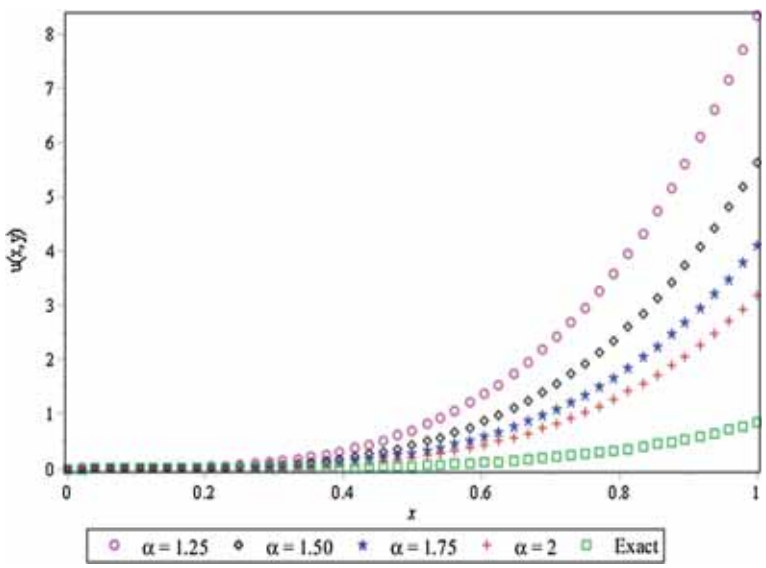

Figure 12. Behaviour of exact and q-FHATM solutions for distinct α when $y = 1 = n, \hbar = -1$ for Example 3.

Proceeding in the same way, we get the solution as

$$u(x, y) = \lim_{n\to\infty} u_n(x, y). \tag{52}$$

5. Numerical results and discussion

It can be easily observed from figures 1–9 that the solution $u(x, y)$ of the space-fractional Helmholtz equation obtained by using q-FHATM and FVIM is almost identical with the exact solution in Examples 1–6. Figures 10–12 show the behaviour of the q-FHATM solution at different values of fractional order $\alpha = 1.25, 1.5, 1.75$ and 2 with the exact solution at $\alpha = 2$ by taking $y = 1, \hbar = -1, n = 1$ for Examples 1–3, respectively. In figure 10, u increases sharply with increasing x and finally coincides with the exact solution at $\alpha = 2$ while in figure 11, u first decreases with increasing x but then increases slowly as α increases and ultimately coincides with the exact solution when $\alpha = 2$. In figure 12, u increases slowly with increasing x and closely approximates with the exact solution when $\alpha = 2$. In figures 13–15, plotting of the $\hbar$-curve are carried out when $n = 1$, $y = 1, \alpha = 2$ for Examples 1–3, respectively. Distinct values of $\hbar$ are chosen to curtail the residual error that guarantees the convergence of the series solution. In figures 16–18, plotting of the n-curve when $x = 1$, $\hbar = -1$, $y = 1$ are executed for Examples 1–3, respectively. They show the behaviour of the numerical solution for distinct values of α. We notice in figures 17 and 18 that as n increases, u also increases but slowly for increasing α. In figure 15, u decreases with increasing n but decreases faster for smaller α. Figures are drawn using Maple package.

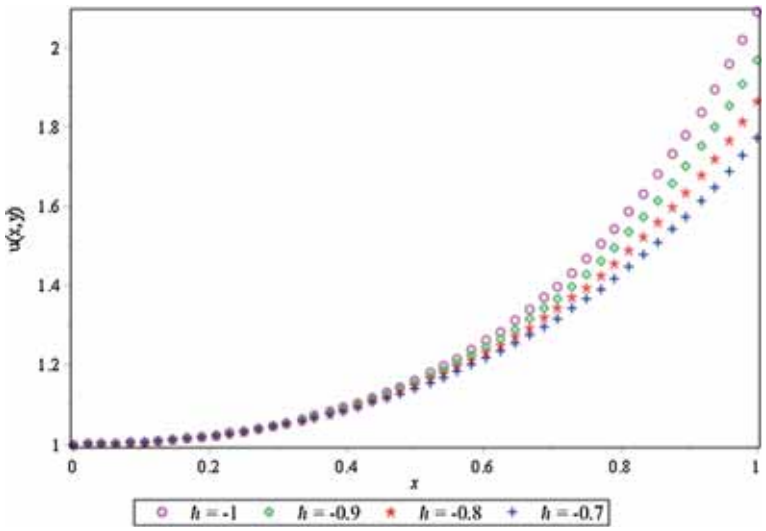

Figure 13. Plot of $\hbar$-curves for $n = 1 = y, \alpha = 2$, for Example 1.

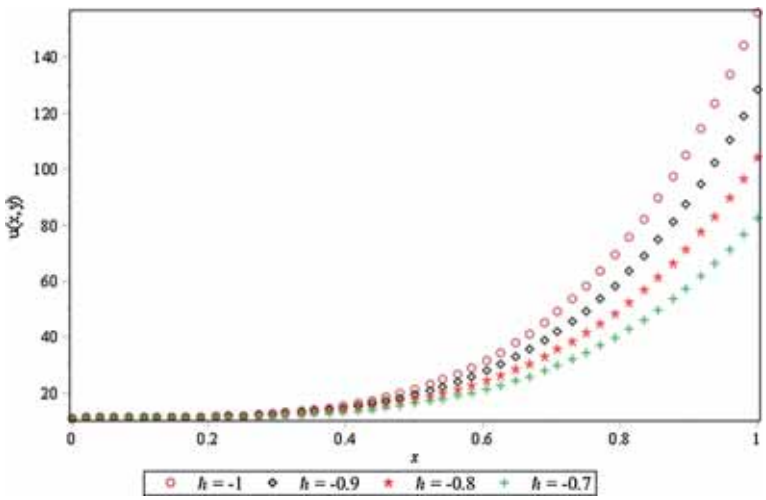

Figure 14. Plot of $\hbar$-curves for $n = 1 = y, \alpha = 2$, for Example 2.

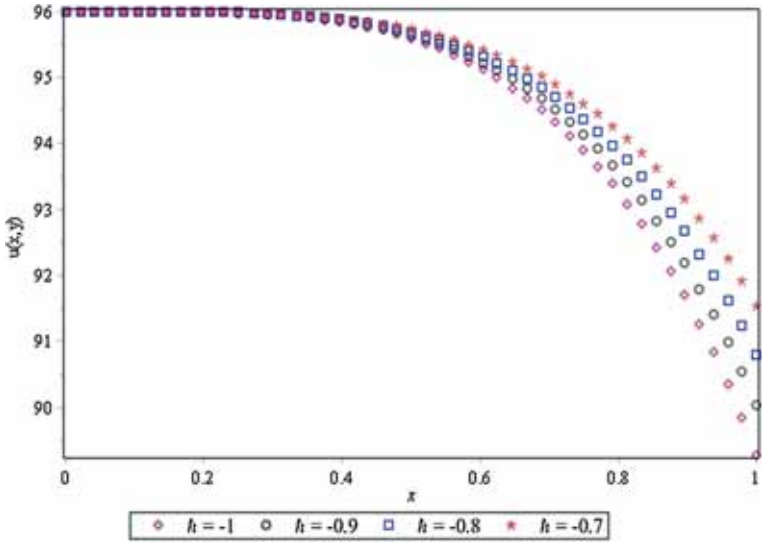

Figure 15. Plot of $\hbar$-curves for $n = 1 = y$, $\alpha = 2$ for Example 3.

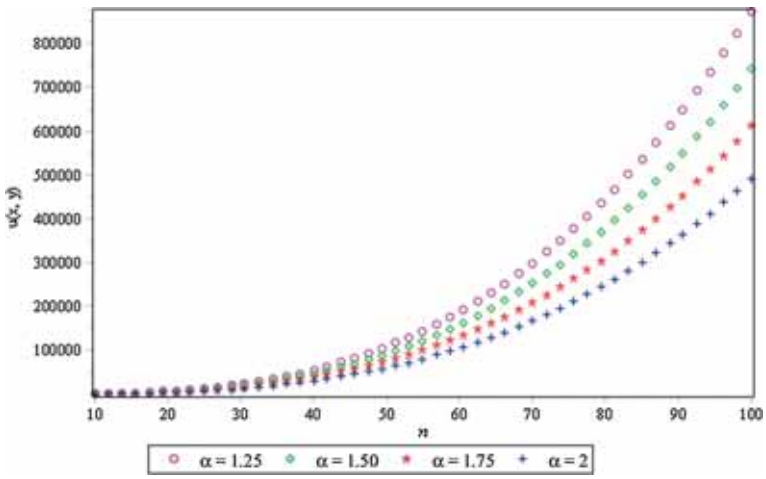

Figure 16. Plot of n-curves for $x = 1 = y$, $\hbar = -1$, for Example 1.

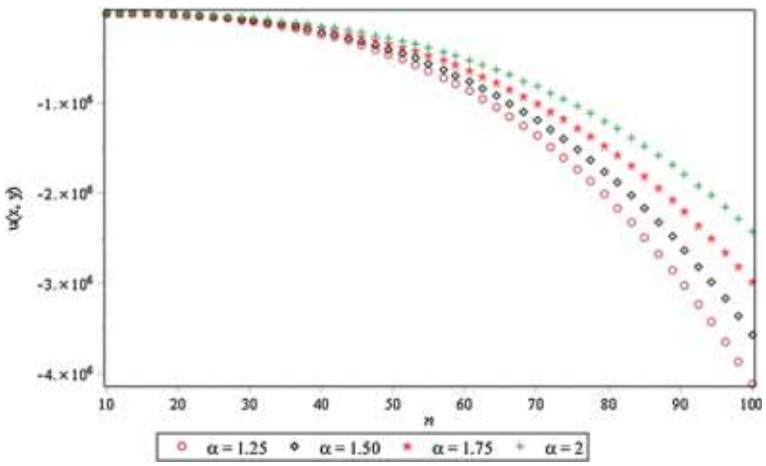

Figure 17. Plot of n-curves for $x = 1 = y$, $\hbar = -1$ for Example 2.

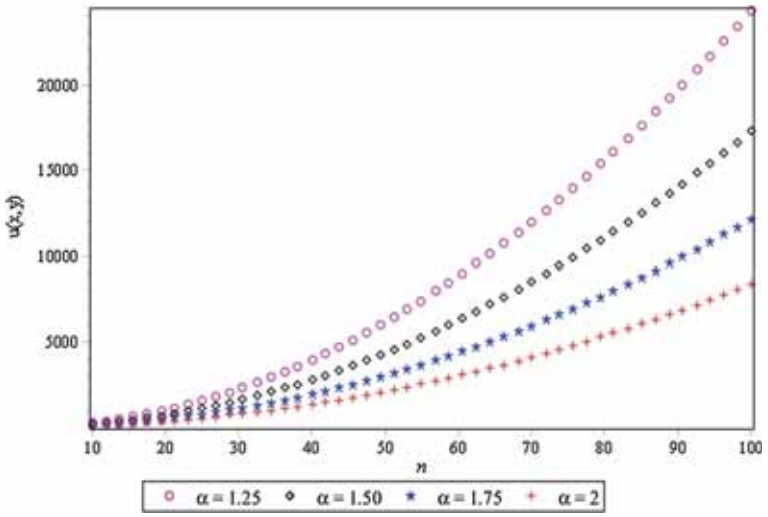

Figure 18. Plot of n-curves for $x = 1 = y$, $\hbar = -1$ for Example 3.

6. Conclusions

In this paper, the proposed numerical algorithms q-FHATM and FVIM are successfully applied to examine the fractional-Helmholtz equation. The outcomes reveal that the results derived using q-FHATM are general, covering the results of FEM, ADM, FDM, DTM, HAM, HPM, FRDTM, etc. as specific cases. Numerical simulations confirm the high accuracy of our results compared to other existing techniques. It is seen that they are capable of reducing the size of calculations and easy to use for both small and large parameters in nonlinear fractional problems. Results inform that FVIM is effective even if lower-order approximations are used. However, the accuracy can be enhanced using more approximations in the solution. It should be noted that FVIM is used directly without using linearisation, perturbation, adomian polynomials or any other restrictive assumptions. It is shown by convergence analysis that the obtained numerical solutions are positive and bounded. Sufficient conditions for the convergence of both methods are established. The q-FHATM contains parameters $\hbar$ and n that manage convergence of series solution. Hence, both the proposed techniques are accurate, highly systematic and attractive and they can be applied for studying any mathematical model of physical importance.

Acknowledgements

The authors are thankful to the reviewers and the editor for their valuable comments in improving the quality of the paper.

References

[1] M Mirzazadeh, *Pramana – J. Phys*. **86**(**5**), 957 (2016)
[2] J H He, *Int. J. Theor. Phys*. **53**(**11**), 3698 (2014)
[3] F J Liu, H Y Liu, Z B Li and J H He, *Therm. Sci*. **21**(**4**), 1867 (2017)
[4] J H He, *Results Phys*. **10**, 272 (2018)
[5] W Zhang and Y Dai, *J. Appl. Math. Phys*. **1**, 18 (2013)
[6] J Y Liu, S H Tsai, C C Wang and C R Chu, *J. Sound Vib*. **275**, 739 (2004)
[7] F Ihlenburg and I Babuska, *SIAM J. Numer. Anal*. **34**, 315 (1997)
[8] S M El-Sayed and D Kaya, *Appl. Math. Comput*. **150**, 763 (2004)
[9] Y K Cheung, W G Jin and O C Zienkiewicz, *Int. J. Numer. Meth. Eng*. **32**, 63 (1991)
[10] N A Khan, A Ara, A Yildirim and E Yuluklu, *World Appl. Sci. J*. **11**(**12**), 1509 (2010)
[11] S Nguyen and C Delcarte, *J. Comput. Phys*. **200**, 34 (2004)
[12] P K Gupta, A Yildirim and K Rai, *Int. J. Numer. Method H* **22**, 424 (2012)
[13] S Abuasad, K Moaddy and I Hashim, *J. King Saud Uni. Sci*. https://doi.org/10.1016/j.jksus.2018.02.002 (2018) (in press)
[14] A Prakash, M Goyal and S Gupta, *Nonlin. Eng*. **8**(**1**), 164 (2019)
[15] K L Wang and K J Wang, *Therm. Sci*. **22**(**4**), 1871 (2018)
[16] J H He, *Int. J. Nonlin. Mech*. **34**(**4**), 699 (1999)
[17] J H He, *Phys. Lett. A* **375**, 3362 (2011)
[18] D Baleanu, H K Jassim and H Khan, *Therm. Sci*. **22**(**1**), S165 (2018)
[19] G Wu and E W M Lee, *Phys. Lett. A* **374**, 2506 (2010)
[20] M A Gondal and M Khan, *Int. J. Nonlin. Sci. Num*. **11**(**12**), 1145 (2010)
[21] Z J Liu, M Y Adamu, E Suleiman and J H He, *Therm. Sci*. **21**(**4**), 1843 (2017)
[22] C Wei, *Therm. Sci*. **22**(**4**), 1723 (2018)

[23] J Singh, D Kumar and R Swaroop, *Alexandria Eng. J*. **55**, 1753 (2016)
[24] S J Liao, *Appl. Math. Comput*. **147**, 499 (2004)
[25] M Y Adamu and P Ogenyi, *Nonlin. Sci. Lett. A* **8**(**2**), 240 (2017)
[26] M Y Adamu and P Ogenyi, *Therm. Sci*. **22**(**4**), 1865 (2018)
[27] Z M Odibat, *Math. Comput. Model*. **51**, 1181 (2010)
[28] M Tatari and M Dehghan, *J. Comput. Appl. Math*. **207**(**1**), 121 (2008)